Rapid Ground Fault Detection in Compensated-Grounded Systems: Design and Testing

Hasan Bayat, Tirath Bains, Amin Zamani
GE Grid Solutions, Canada
hasan.bayat@ge.com

Matthew Webster, Jesse Rorabaugh, Arturo Torres
Southern California Edison, USA
matthew.webster@sce.com

Abstract— **The use of Arc Suppression Coils (ASCs) has been proposed as a means to reduce the possibility of a fire ignition by ground faults. The ASC compensates for the capacitive component of the fault current, hence resulting in a very small ground fault current, which reduces the probability of ignition from a ground fault. The reduced fault current, however, leads to a new challenge of ground fault detection and direction (reverse or forward); in other words, traditional directional elements are rendered inadequate to reliably identify faulted feeders when fault currents are small. Transient Ground Fault Detection (TGFD) is a patented algorithm that can reliably detect ground faults and identify its direction in compensated-grounded systems. This study describes design considerations for the rapid ground fault detection in compensated-grounded systems. Further, it examines the effectiveness of the TGFD function for fire mitigation applications in compensated-grounded systems. The results of a comprehensive set of tests show satisfactory performance of the TGFD function for fire mitigation applications, i.e., very low fault currents.**

Keywords— ***Arc Suppression Coil, fire mitigation, ground fault, Petersen coil, Rapid Earth Fault Current Limiter, Transient Ground Fault Detection.***

I. INTRODUCTION

Ground faults have been identified as one of the catalysts in starting a fire ignition. In ungrounded systems, the level of fault current is greatly reduced; however, the fault arc due to the charging capacitance of the system can still be enough to start ignition. This has led to a renewed interest towards compensated-grounded systems using inductive coils. The inductive coil is referred to as either Petersen coil or Arc Suppression Coil (ASC) in the literature, which are used interchangeably in this paper. Depending on the compensation level, the ASC compensates for the capacitive component of the fault current, thereby resulting in a very small resistive fault current. In some cases, a Residual Current Compensation (RCC) module is also utilized to compensate for the resistive component of the fault current, hence further reducing the ground fault current/energy; this, in turn, reduces the probability of ignition from a ground fault in the feeder by a about 90 percent [1]. The reduced fault current, however, leads to a new challenge of detecting the fault current direction (i.e., reverse or forward). Due to the small value of ground fault currents, the traditional directional elements including Wattmetric function (32N) are rendered inadequate to reliably identify the faulted feeder.

Transient Ground Fault Detection (TGFD) is a patented algorithm which identifies the direction of the fault in ungrounded, resistive-grounded, and resonant-grounded systems (with or without RCC). The TGFD operation does not require any special equipment, and it can be added to GE Universal Relays (UR) as a firmware upgrade. Moreover, it uses regular sampling frequency that is utilized for other protection functions/elements.

The TGFD function uses a different frequency than the power system frequency to determine the fault direction in a faulted feeder. Consequently, its dependency on the ground fault current magnitude is low and can operate for faults with very small current magnitudes. This means that the function can be applied in ungrounded, resistance grounded, and compensated-grounded systems (with arc suppression coils). The TGFD function has mainly been used for grid reliability purposes as it can avoid unnecessary interruption caused by temporary faults. This study, however, intends to examine the application of the TGFD function for fire mitigation applications in compensated-grounded systems. The paper provides the methodology, results, and findings of testing and evaluation of GE's TGFD algorithm for application in Southern California Edison's (SCE) compensated-grounded distribution systems.

The rest of this paper is organized as follows. It will first provide an overview of the power system grounding schemes along with the grounded system behaviors during ground faults. Then, the protection of compensated-grounded systems will be discussed followed by operating fundamentals of the TGFD function; some of the design considerations including Current Transformer (CT) selection criteria are also described in this section. Finally, the results of the hardware-in-the-loop testing for a realistic distribution substation (with two feeders) are presented to demonstrate the effectiveness of the TGFD function. A detailed model of a utility distribution system that is grounded using the ASC is created in the Real-Time Digital Simulator (RTDS), and the RTDS is interfaced with three relays whose TFGD functions are properly set. A comprehensive set of tests is conducted under various conditions (different fault resistances, fault locations, compensation level, etc.) to evaluate the effectiveness of the TGFD element implemented in GE UR relays.

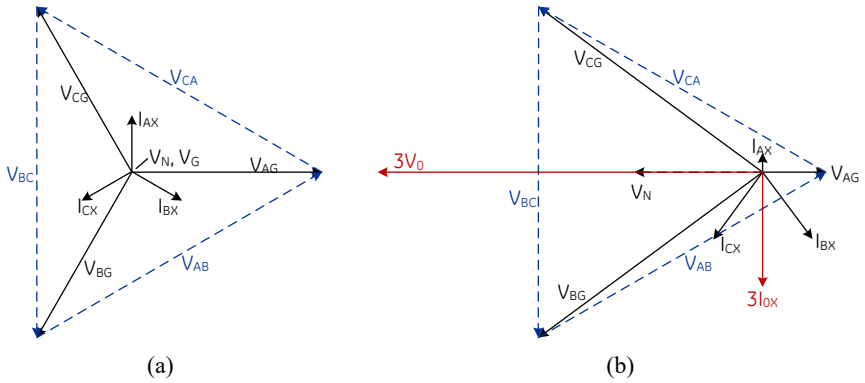

Figure 1- (a) Phasors in pre-fault conditions (b)Phasors during a SLG fault in impedance/ungrounded system.

II. POWER SYSTEM GROUNDING

Solidly grounded systems are widely used in North America. Due to high fault current in solidly ground systems, the identification of the faulted feeder can be easily accomplished using a phase overcurrent relay. Moreover, the overvoltage(s) caused by single-line-to-ground (SLG) faults are smaller in solidly grounded systems. However, the arcing caused by high fault current presents a significant risk to the public, including possibility of a fire ignition. Apart from solidly grounded systems, other types of grounding mechanisms are:

- Ungrounded system,
- Resistance grounded system, and
- Resonant grounded systems (via Petersen coil).

In all the above listed grounded systems, the loads are always connected between phases. Therefore, during normal operation, there is almost no (very small) zero-sequence current as can be seen from Figure 1(a). During a single-phase to ground fault, the phase to ground voltage of the faulted phase declines while the phase to ground voltages of the healthy phases rise. As a result, significant residual voltage ($3V_0$) builds up as shown in Figure 1(b). Now, due to the unbalanced phase to ground voltages, the charging current drawn by the phase to ground capacitances is also unbalanced which results in net residual current in the system ($3I_0$). Also, it can be observed from Figure 1(b) that the phase to phase voltages of the system remain balanced and the loads keep operating normally during a single-phase to ground fault.

Traditionally, the Wattmetric ground fault element (32N) which essentially is a zero-sequence directional element has been utilized to identify the faulted feeder in non-solidly grounded systems as explained below.

A. Ungrounded Systems

Figure 2(a) shows an ungrounded system with a solid single-phase to ground fault in Feeder 2. It can be seen from this figure that the charging current of the healthy phases of the whole system passes through the fault point. As a result, the residual current measured by CT2 is the negative of the charging current of the whole system minus the charging current of Feeder 2. Thus, the residual current measured by CT2 will lag $3V_0$ by approximately 90º. In contrast, the residual current measured by CT1 is the charging current of Feeder 1 and will lead $3V_0$ by approximately 90º. this means that the faulted feeder can be identified using the Wattmetric element.

B. Resistance-Grounded Systems

In resistance-grounded networks, the neutral point is grounded using a resistor. If the grounding resistance is low, then the fault current is high, while the over-voltage in healthy phases is relatively small. If the grounding resistance is high, then the fault current is low; however, the over-voltage in healthy phases is high. In this respect, the high-resistance-grounded systems are closer to ungrounded network, while low-resistance-grounded systems are closer to solidly grounded networks.

Figure 2(b) shows a solid single-phase to ground fault in Feeder 2 in a resistance-grounded network. For these systems, the charging current as well as the current through the neutral point of the system (I_N) pass through the fault point of the system. Consequently, the residual current measured by CT2 is the phasor sum of I_N and the negative of the charging current of the whole system excluding the charging current of Feeder 2. On the other hand, the residual current measured by CT1 will be the charging current of Feeder 1 only. Therefore, for a faulted feeder, the residual current will lag $3V_0$ by more than 90º but less than 180º, while for healthy feeder, the residual current will lead $3V_0$ by 90º approximately. Alternatively, it can be stated that for a faulted feeder, the residual current will lead $-3V_0$ by less than 90º while for a healthy feeder, the residual current will lag $-3V_0$ by 90º approximately.

The angle by which residual current in faulted phase would lead $-3V_0$ depends on the zero-sequence admittance of the network and the grounding resistance, but is independent of the fault resistance. With higher grounding impedance, the angle by which the residual current of the faulted phase would lead $-3V_0$ will increase. Nevertheless, by knowing the key system parameters such as grounding resistance and charging current of the system, the Wattmetric element can be set properly to identify the faulted feeder in resistance-grounded networks.

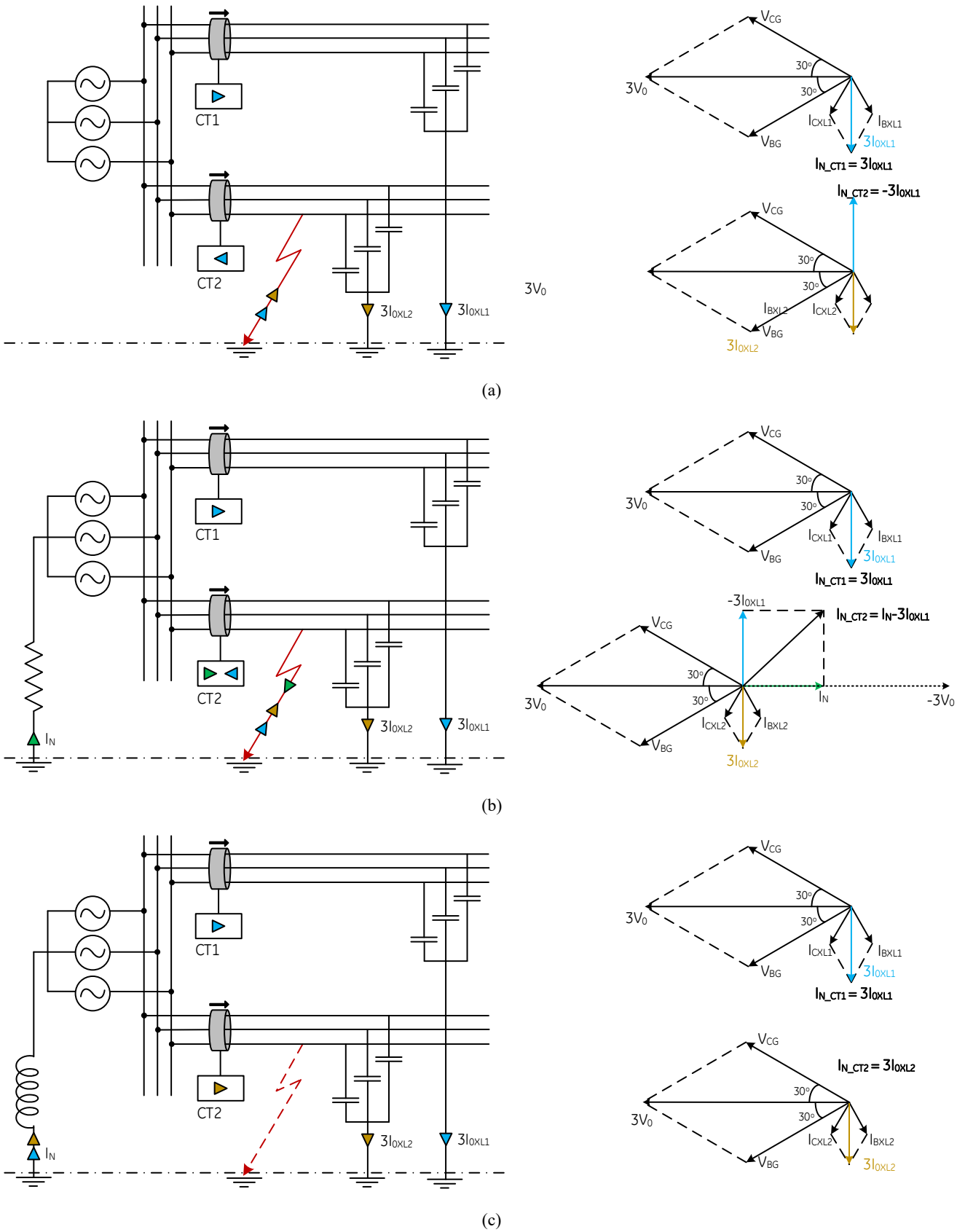

Figure 2- Phase relation between residual voltage and current in a healthy and a faulted feeder for different types of the system grounding

C. *Resonant-Grounded Systems*

In resonant-grounded (or Petersen-coil-grounded) systems, the neutral point is grounded through an inductor. It can be seen that from analysis presented before in ungrounded or resistively grounded networks, the fault current cannot be reduced below the charging current of the system, which actually can rise by $\sqrt{3}$ times due to over-voltage in healthy phases during a solid single-line to ground fault. This charging current could present as ignition risk. Any further decrease in the fault current (below the charging current) can only be accomplished through Petersen-coil-grounded systems. The grounding inductor compensates the capacitive charging current thus reducing the fault current. Depending upon the compensation level, the fault current in Petersen-coil-grounded system can be:

1- Inductive (over-compensation),
2- Capacitive (under-compensation), or
3- Zero (full compensation).

Figure 2(c) shows a resonant compensated-grounded system with a solid single-phase to ground fault, where it can be seen that the grounding inductor compensates fully for the capacitive charging current; as a result, there is no current at the fault point. Due to the ability of resonant-grounded networks to limit the fault currents to a low value, it reduces the chance of fire ignition by about 90% [1]. However, detecting the faulted feeder in resonant grounded systems becomes challenging for Wattmetric element.

It can be seen from Figure 2(c) that the residual current measured by CT1 and CT2 are the charging currents of their respective feeders with identical phase relationship with $3V_0$. Although there can be a small resistive fault current owing to resistance of the Petersen coil, and conductance of the system, it might not be reliable enough to discriminate between healthy and faulted feeder. Moreover, by using residual current compensation (RCC) device at the grounding point, this small resistive fault current can be removed altogether. Thus, detecting a faulted feeder using Wattmetric element becomes very difficult, and a need arises to have a robust element like TGFD which can reliably detect the faulted feeder in ungrounded, resistance-grounded, and Petersen-coil-grounded systems (for all compensation levels).

A comparison of different grounding systems based on three main criteria is provided in Table I.

Table I- Grounding systems comparison

Attribute	Grounding Systems				
	Solidly Grounded	Ungrounded	Resistance		Resonant Grounded
			High	Low	
Transient Overvoltage	Low	High	Medium/ High	Low	Medium
Continuous operation with SLG fault	No	Yes	Yes	No	Yes
Self-Extinguish SLG Fault	No	Yes	Yes	No	Yes

III. PROTECTION OF COMPENSATED-GROUNDED SYSTEMS

Ground fault current can be small in a Petersen-coil-grounded system depending on compensation level and whether an RCC is coupled with the ASC. The impact of the low fault current is that identifying the faulted feeder becomes challenging since there is not much current for overcurrent elements to operate. As discussed above, Watttmetric and Transient Ground Fault Detection (TGFD) functions are the two elements that can alleviate the faulted feeder identification in these types of systems.

A. *Neutral Voltage Rise*

During a ground fault incident in a Petersen-coil-grounded system, the neutral voltage rises to a value which is determined

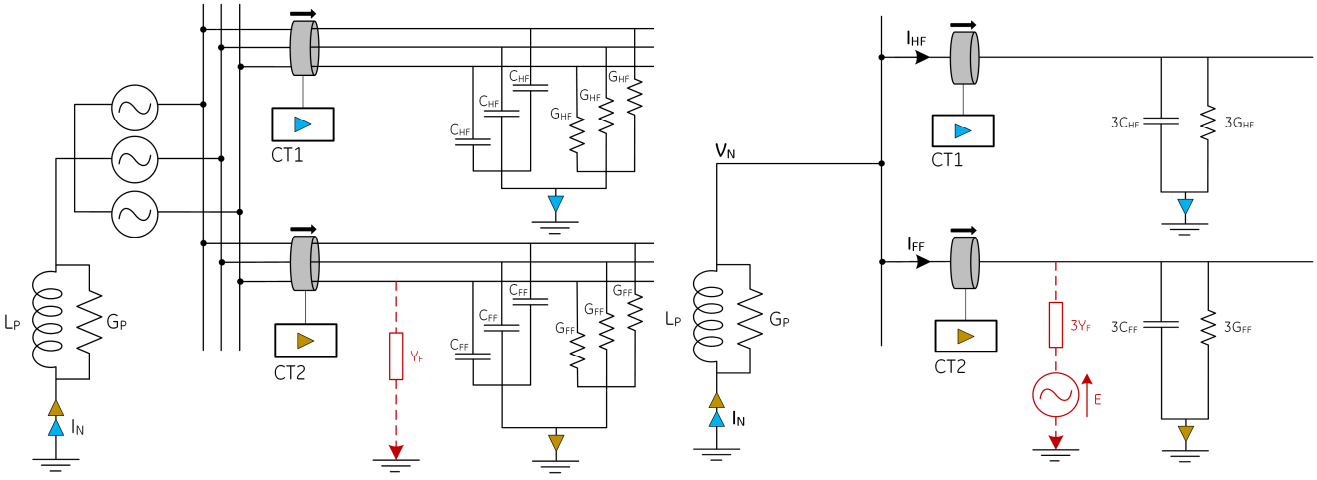

(a) (b)

Figure 3- (a) Generalized system model (b) Zero-sequence model of the generalized system

by the admittance of the system and the ASC. The neutral voltage in this situation can be calculated using:

$$0 = Y_P V_N + Y_A V_A + Y_B V_B + Y_C V_C \quad (1)$$

Where Y_P, Y_A, Y_B, and Y_C are the Petersen coil and phase-to-ground admittances. According to the notations presented in Figure 3 and assuming a balanced system, one can write

$$\begin{aligned} V_A &= V_N + E \\ V_B &= V_N + a^2 E \\ V_C &= V_N + aE \end{aligned} \quad (2)$$

$$Y_A = Y_B = Y_C = Y_S = G_S + j\omega C_s \quad (3)$$

Where Y_S is the phase admittance of the entire system which in turn is comprised of conductance (G_S) and susceptance (ωC_s). Then, one can obtain:

$$V_N = -\frac{Y_A + a^2 Y_B + a Y_C}{Y_P + Y_A + Y_B + Y_C} E \quad (4)$$

Where E is the nominal phase voltage; If admittance of the three phases are exactly equal, the V_N will be zero during normal operation of the system. However, when a fault takes place, the admittance of the fault will be in parallel with the admittance of the faulted phase. Assuming a balanced system and the fault on phase A, the neutral voltage can be calculated as

$$\begin{aligned} V_N &= -\frac{Y_S\left(\overbrace{1 + a + a^2}^{=0}\right) + Y_F}{Y_P + 3Y_S + Y_F} E \\ &= -\frac{Y_F}{G_P + 3G_S + \frac{1}{j\omega L_P} + j\omega 3C_S + Y_F} E \end{aligned} \quad (5)$$

Where Y_F is the admittance of the fault which is also assumed to be purely resistive and expressed in terms of its conductance (G_F). Figure 4(a) shows the equivalent circuit of (5). Assuming a resistive fault, Equation (5) can be rewritten as

$$V_N = -\frac{G_F}{G_P + 3G_S + G_F - j\left(\frac{1}{\omega L_P} - 3\omega C_S\right)} E \quad (6)$$

It can be deduced from Equation (6) that the voltage rise of neutral is a very reliable indicator of the fault in the system covering fault admittances as low as the shunt admittances of the network and Petersen coil (i.e., very high fault resistance). Figure 4(b) shows the neutral voltage rise of the study system due to single phase faults with different fault resistance.

B. Feeder Models

The phase-frequency response of line admittances (both healthy and faulted feeders) are presented in this section. The phase-frequency characteristics of the faulted and healthy lines are distinctive within a frequency band which is the basis for the operation of the TGFD function. the healthy feeder exhibits capacitive behavior while the faulted feeder exhibits an inductive characteristic within the frequency band of interest. The frequencies associated with distinctive behavior of faulted and healthy feeders are derived in this section.

1) Healthy Feeder Model

PI line models are used to model the feeder in a distribution system. Zero-sequence admittance of the healthy line seen by the relay is calculated as

$$Y_{HF} = G_{HF} + jB_{HF} \quad (7)$$

Where G_{HF} and B_{HF} are the conductance and susceptance of the healthy feeder, respectively. It should be noted that the healthy feeder is a representation of the rest of the system and can be comprised of multiple feeders. The phase-frequency characteristic of the healthy line is shown in Figure 5. The frequencies at which the sign of the phase angle of the healthy line admittance changes are [2]:

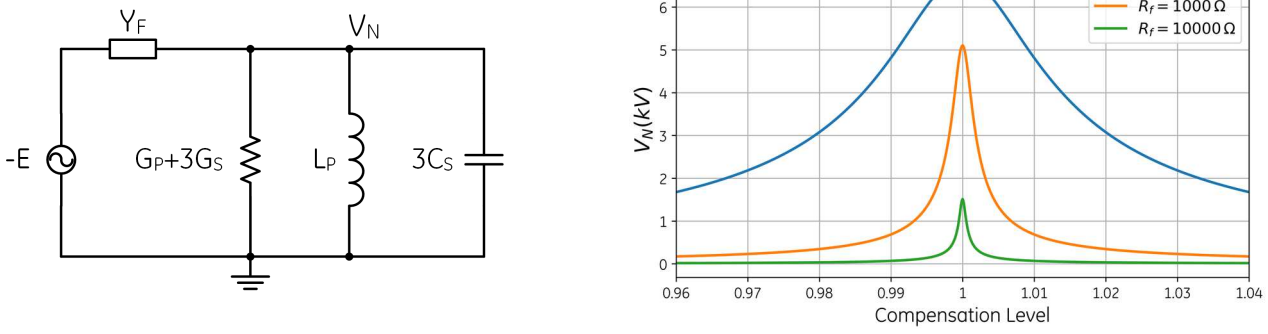

(a) (b)

Figure 4- (a) Zero-sequence network (b) Neutral voltage with respect to compensation level

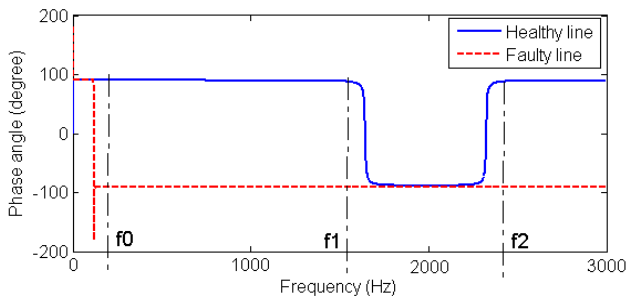

(a)

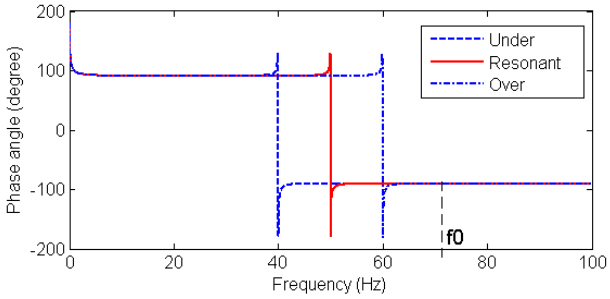

(b)

Figure 5- Phase-frequency response of line admittances (healthy feeder vs faulted feeder)

$$f_1 \approx \frac{c}{\sqrt{2}\pi l} \quad (8)$$

$$f_1 \approx \frac{c}{\pi l} \quad (9)$$

Where c is the speed of electromagnetic wave (i.e., light speed). According to Figure 5(a), the phase angle of the admittance of the healthy line is +90˚ (capacitive) in low frequencies and will change to -90˚ (inductive) between f_1 and f_2; again, it will becomes +90˚(capacitive) in higher frequencies.

2) Faulted Feeder Model

Based on Figure 3(b), the current of the healthy feeder (I_{HF}) can be calculated as

$$I_{HF}(\omega) = (3G_{HF} + j\omega 3C_{HF})V_N \quad (10)$$

While that of the faulted feeder (I_{FF}) is calculated using

$$\begin{aligned} I_{FF}(\omega) &= I_N(\omega) - I_{FF}(\omega) \\ &= -V_N\left(G_P + \frac{1}{j\omega 3L_P}\right), \\ &\quad - (3G_{HF} + j\omega 3C_{HF})V_N \end{aligned} \quad (11)$$

Considering the following relationship

$$Y_S(\omega) = Y_{HF}(\omega) + Y_{FF}(\omega) \quad (12)$$

And defining the compensation level at the power system frequency as

$$K_C = \frac{I_L}{3I_{C_S}} = \frac{\frac{1}{j\omega_n L_P}V_N}{j\omega_n 3C_S V_N} = \frac{-1}{\omega_n^2 3C_S L_P} \quad (13)$$

Equation (*11*) can be rewritten as

$$\begin{aligned} I_{FF}(\omega) = -V_N\Big(&G_P + (3G_S - 3G_{FF}) \\ &+ j\omega 3C_S\left[\frac{3C_S - 3C_{FF}}{3C_S} + \left[K_C\left(\frac{\omega_n}{\omega}\right)\right]^2\right]\Big) \end{aligned} \quad (14)$$

Where ω_n is the nominal system frequency in rad/sec. Therefore, the imaginary component of *(14)* becomes negative (inductive) at

$$f_3 = \sqrt{\frac{K_C C_S}{C_S - C_{FF}}} f_n \quad (15)$$

Where f_n the nominal system frequency in 'Hz'; f_3 is the frequency at which the phase angle of the admittance of the faulted feeder changes to inductive from capacitive; this frequency is highly correlated with the power system frequency (its magnitude depends on the system admittances). For practical distribution substations with several feeders/circuits, the capacitance of the faulted feeder constitutes only a relatively small portion of the capacitance of the whole system; thus, f_3 will be closer to the system nominal frequency.

C. Transient Ground Fault Detection (TGFD) Function

As stated earlier, the TGFD function identifies the direction of the fault in ungrounded, resistive grounded, and resonant-grounded systems [2]. The operating quantity for the TGFD function is zero-sequence current and zero-sequence voltage of the feeder at a frequency different than the power system frequencies. The frequencies of interest are 264Hz and 220Hz for 60-Hz and 50-Hz power systems, respectively. These frequency components are extracted and utilized to calculate transient reactive power. The TGFD operation does not require any special equipment, and it is added to the relay as a firmware update. Further, the sampling frequency does not need to be high, and the regular sampling frequency used for other protection functions does suffice.

D. TGFD Background

The frequency that can be used to differentiate between a healthy and faulted line is not an absolute value. It is a frequency band which stretches from $f_0 \approx 75$Hz to $f_1 \approx 1500$Hz (see Figure 5) [2]. The distinctive feature between the faulted and healthy lines is the phase angle of the zero-sequence admittance seen by the relay for the frequencies between f_0 and f_1 [3]. Figure 5(a) shows the phase-frequency response of the admittance seen by the relay

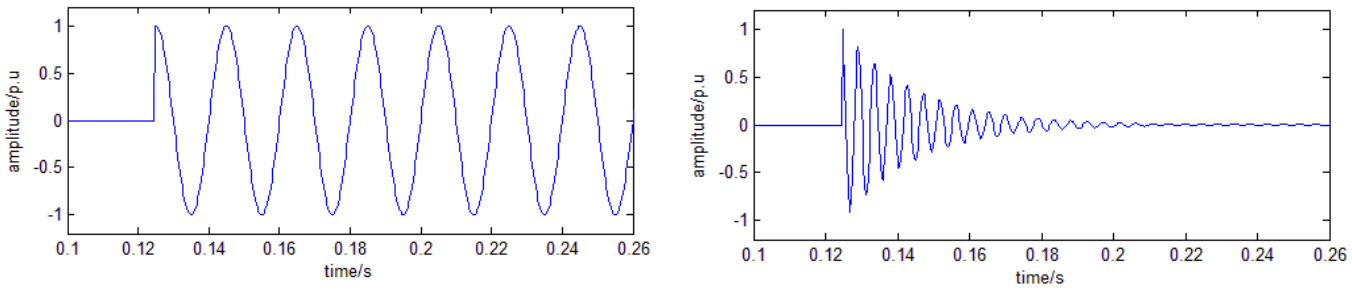

(a) (b)

Figure 6- (a) Zero-sequence current seen by the relay (fault at t~0.12s), and (b) Transient 264-Hz current caused by a SLG fault

in a healthy line versus that of a faulted line, while Figure 5(b) shows the shift in phase-frequency response of the admittance of the faulted line for frequencies below f_0.

Any frequency residing between f_0 and f_1 could be used to determine fault direction. However, the following are the three main reasons behind the selection of 264Hz (for a 60-Hz system):

1- Accurate measurement of 264Hz does not require extra hardware and the existing GE URs hardware is capable of measuring this frequency accurately.

2- Measuring 264Hz does not require higher sampling frequency and the existing sampling rate in GE URs is enough for measuring this frequency accurately.

3- This frequency is an inter-harmonic and does not exist in the power system. By using this frequency, the multiples of fundamental frequency are avoided.

The zero-sequence current and zero-sequence voltage values measured by the relay prior to SLG faults are zero (for a balanced system) and small (in an unbalanced system). However, when a fault occurs, the zero-sequence current and zero-sequence voltage rise to higher values immediately or gradually depending on the fault impedance and Point on Wave (POW). The amount of increase in current caused by the fault affects the transient reactive power measured by the relay. Figure 6(a) shows the zero-sequence current seen by the relay before and after a SLG fault in a balanced system, where the fault happens at the peak of the phase voltage (POW = 90°), causing a sharp jump in the zero-sequence current. Figure 6(b) shows the filtered zero-sequence current at the output of 264Hz filter. It is noted that the transient nature of the 264-Hz current component gradually decays to zero.

The transient reactive power is calculated from the 264Hz components of the zero-sequence current and zero-sequence voltage. If the calculated reactive power is negative and lower than the dynamically calculated threshold, then the fault is declared as Forward (feeder is faulted). Since, the magnitude of the 264-Hz current component is affected by the instance at which the fault happens as well as the fault impedance, there is a possibility that the transient reactive power (Q) measured by the relay will not be enough to cause the operation of the TGFD element, e.g., when the fault happens exactly at zero crossing of

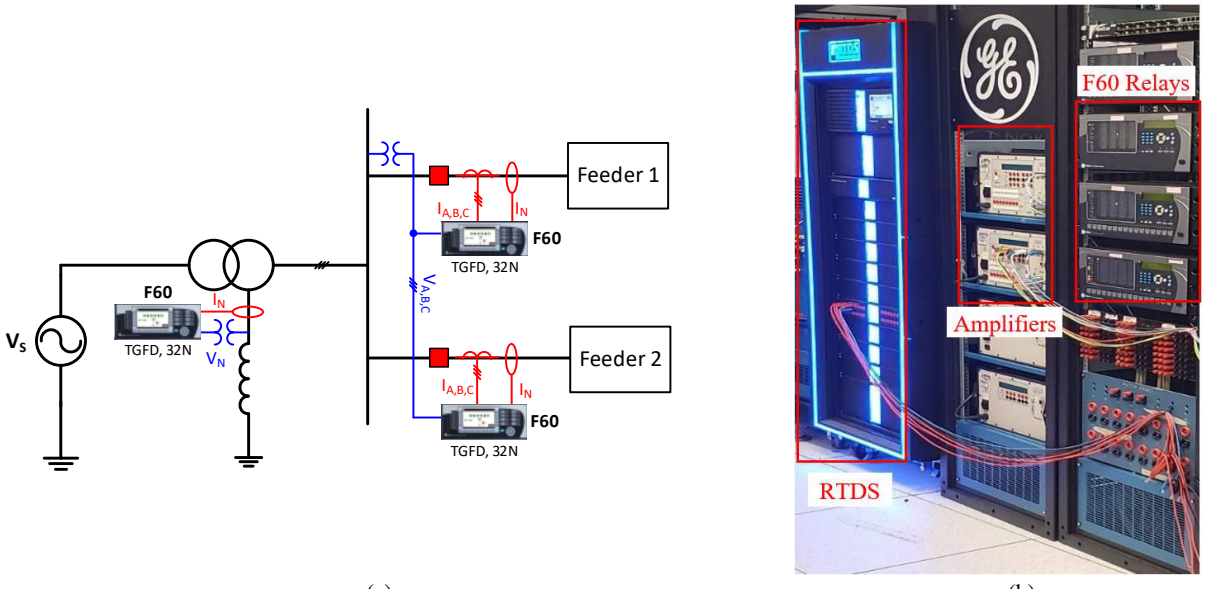

(a) (b)

Figure 7- (a) Simplified SLD of the study system, and (b) HIL test setup at the GE Digital Integration Lab

the phase voltage. In such a case, the transient active power (P) is expected to operate, leading to higher reliability of the overall function [4]. As such, when the transient Q is small, the TGFD function automatically switches to transient P. The transient P is obtained from unfiltered zero-sequence current and voltage which includes fundamental component and all other transients. The operation logic based on transient P is similar to that of the transient Q. The calculated transient P is compared against negative and positive thresholds. If it is lower than the negative threshold, the fault will be declared as forward while if the measured transit P is greater than the positive threshold, the fault will be classified as reverse.

E. Current Transformer Selection

The objective of this study is wildfire prevention due to power line failures. ASC is used to limit the fault current in case of a ground fault and decrease the likelihood of an ignition. In this study, the fault current of interest is 0.5A. As a result, the Current Transformer (CT) of interest must be able to measure a 0.5A resistive fault current accurately. The 0.5A fault current detection comes from SCE's requirement for fault detection in Petersen-coil-grounded systems. The testing was performed assuming a 50:5 CT with 0.15S accuracy class for feeder relays. For the substation relay, a 20/5 CT with the accuracy of 0.15S was assumed.

Two CT types were considered in this study: Holmgren CTs and Core-Balanced CTs. Since the required CT ratio is 10, the Holmgren CT will have a high circulating current at its secondary due to the load current. Secondly, there are concerns about the exact match between the CTs of Holmgren connection which may cause some spill of load current into zero sequence current. Therefore, core-balanced zero-sequence CTs were selected for the TGFD application since it does have a small secondary current in normal operating mode of the system and can be found in lower CT ratios.

IV. TEST SETUP AND PROCEDURES

In this section, the results of the Hardware-in-the-Loop (HIL) testing using the Real-Time Digital simulator (RTDS) are presented and discussed. Comprehensive sets of tests were executed to evaluate the performance of the TFGD function in a compensated-grounded distribution system (using Petersen coil) under various fault scenarios. The results of a selected number of test cases are described in more details to provide additional information on the TGFD function capability and sensitivity.

A. Test Setup

A simplified Single-Line Diagram (SLD) of the system under study is shown in Figure 7(a) ("study system"). As can be seen in this figure, the study system has two feeders, namely, Feeder 1 and Feeder 2. A detailed model of the study system has been created in the RTDS. The location of the physical/hardware devices (relays) on the feeder and the substation are indicated in the figure; these devices are part of the HIL testing.

The control hardware-in-the-loop testbed was developed in the GE Digital Integration Lab; Figure 7(b) shows a picture of the lab test setup. The rack on the right side of the picture encloses all three relays (F60 UR). The middle rack embeds amplifiers, while the left-side rack is the RTDS.

Table II- A summary of test results for fully compensated scenario

Rapid Earth Fault Current Limiter (REFCL) - SCE - Full Compensated							
Case ID	**Faulted Feeder**	**Rf (Ohm)**	**Faulted Phase**	**POW (deg)**	**Flt Current (A_{RMS})**	**Feeder 1 TGFD (ms)**	**Feeder 2 TGFD (ms)**
1001	FEEDER 1	0	A	0	1.55	FW/11ms	RE/11ms
1002	FEEDER 1	0	A	45	1.55	FW/9ms	RE/11ms
1003	FEEDER 1	0	A	90	1.525	FW/9ms	RE/11ms
1004	FEEDER 1	0	A	135	1.54	FW/9ms	RE/10ms
1006	FEEDER 1	10,000	A	0	0.522	FW/8ms	RE/542ms
1007	FEEDER 1	10,000	A	45	0.519	FW/8ms	RE/540ms
1008	FEEDER 1	10,000	A	90	0.521	FW/76ms	RE/540ms
1009	FEEDER 1	10,000	A	135	0.519	FW/73ms	RE/54ms
2001	FEEDER 2	0	A	0	1.59	RE/10ms	FW/9ms
2002	FEEDER 2	0	A	45	1.59	RE/11ms	FW/9ms
2003	FEEDER 2	0	A	90	1.55	RE/11ms	FW/9ms
2004	FEEDER 2	0	A	135	1.58	RE/13ms	FW/11ms
2006	FEEDER 2	10,000	A	0	0.488	RE/545ms	FW/55ms
2007	FEEDER 2	10,000	A	45	0.488	RE/543ms	FW/53ms
2008	FEEDER 2	10,000	A	90	0.493	RE/545ms	FW/54ms
2009	FEEDER 2	10,000	A	135	0.492	RE/547ms	FW/57ms
5001	FEEDER 1	0	B	0	1.61	FW/11ms	RE/11ms
5002	FEEDER 1	0	C	0	1.75	FW/10ms	RE/12ms
5003	FEEDER 1	8,000	B	0	0.585	FW/55ms	RE/540ms
5004	FEEDER 1	7,000	C	0	0.69	FW/79ms	RE/55ms
5005	FEEDER 2	0	B	0	1.71	RE/11ms	FW/9ms
5006	FEEDER 2	0	C	0	1.84	RE/12ms	FW/10ms
5007	FEEDER 2	8,000	B	0	0.592	RE/542ms	FW/51ms
5008	FEEDER 2	7,000	C	0	0.701	RE/66ms	FW/62ms

FW: Forward; RE: Reverse

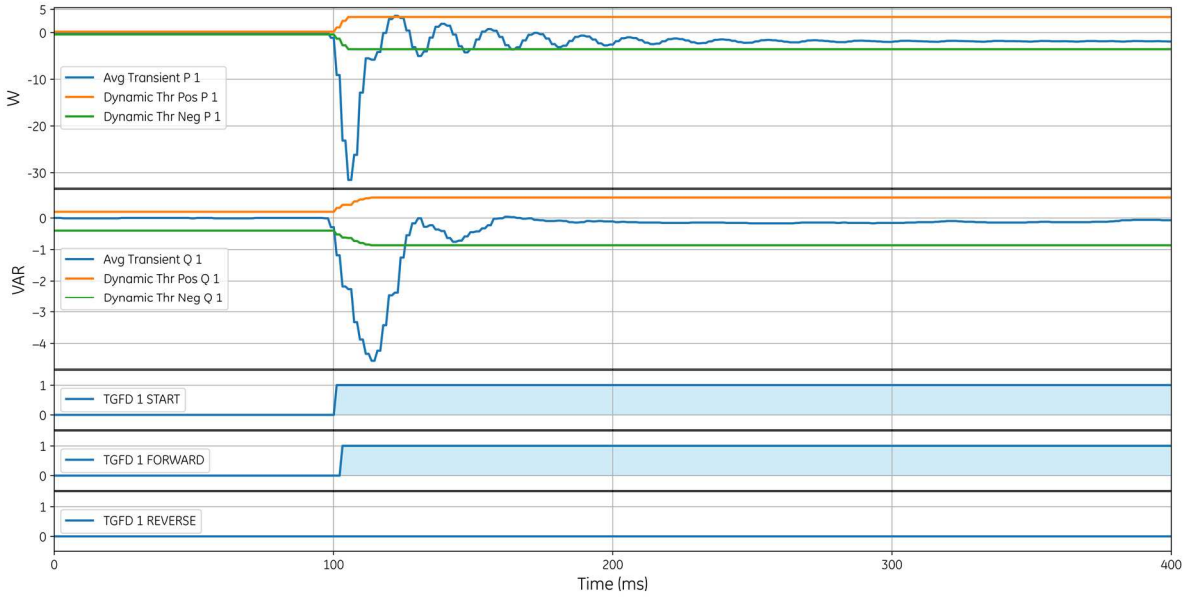

(a)

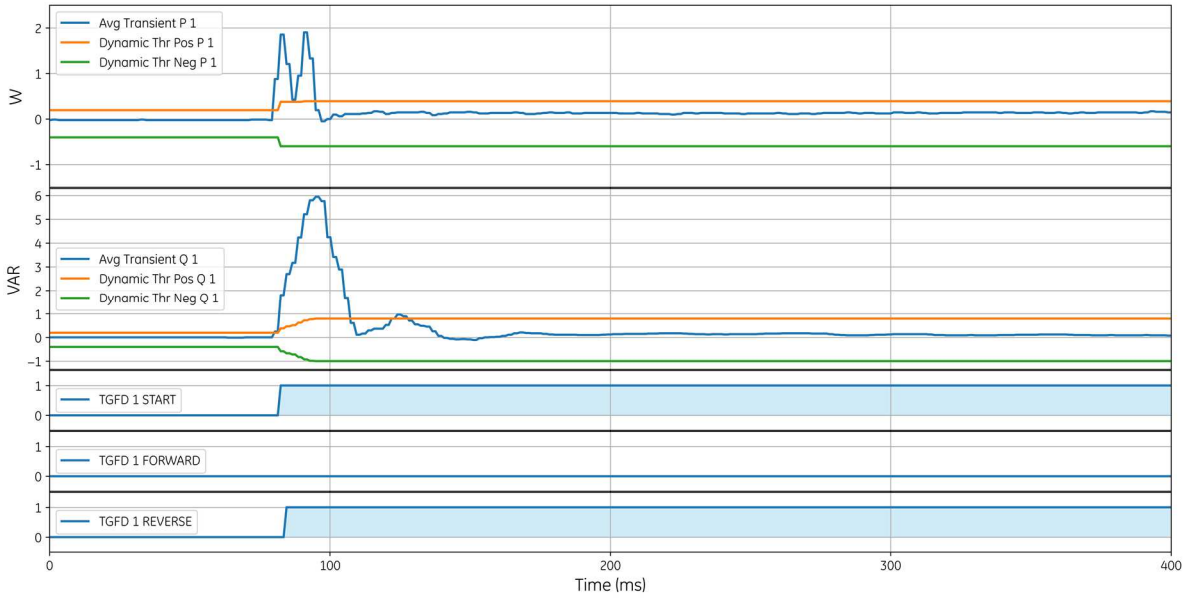

(b)

Figure 8- Low-impedance fault on Feeder 1: (a) faulted feeder and (b) healthy feeder

B. Test Cases

This section outlines the cases that have been tested to analyze the performance of the TGFD function under various fault scenarios and transient incidents. In the preparation of the test cases, various factors that can potentially impact the TGFD performance are considered; the main factors include:

- Fault location
- Fault resistance;
- Point of Wave (POW);
- Grounding compensation level;
- Feeder loading;
- Faulted phase; and
- Load trip (transient)

It should be noted that the test cases are chosen in a manner that worst-case scenarios are covered while the total number of cases is managed. Tests were carried out for full/resonant grounding, 80% compensated system (under-compensation) and 120% compensated system (over-compensation). The number of tests performed in this study is more than 140 tests.

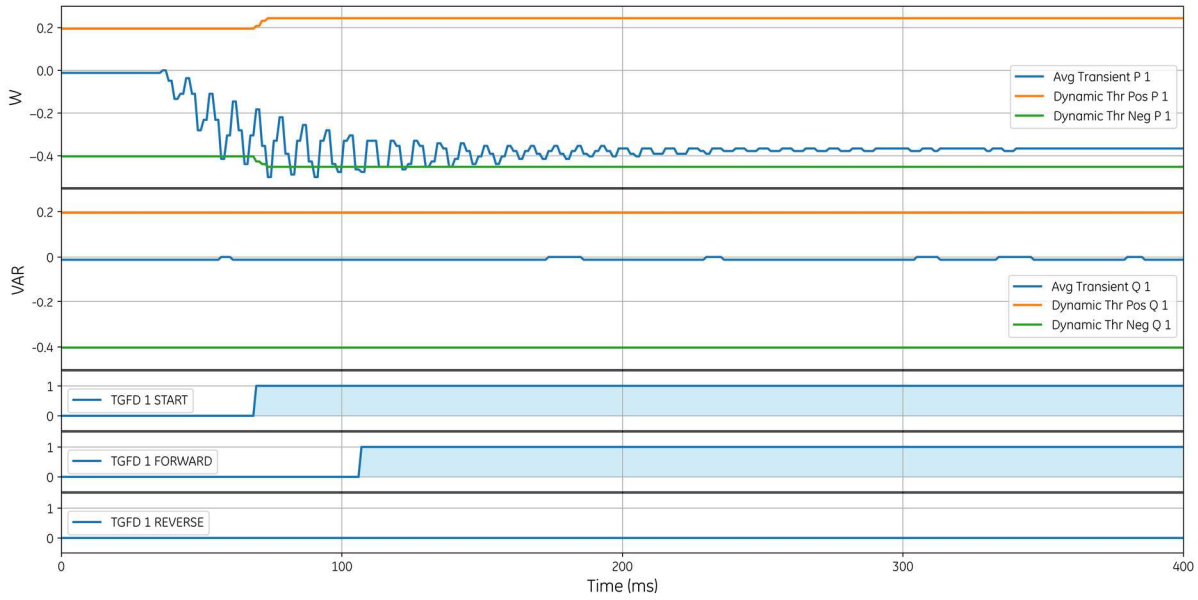

(a)

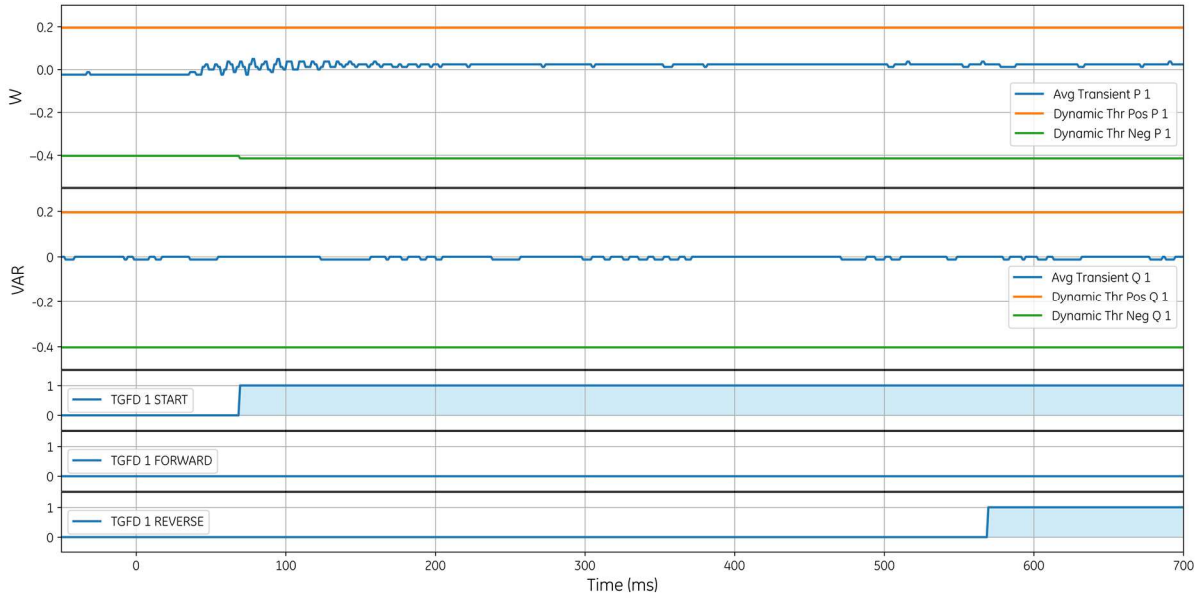

(b)

Figure 9- High-impedance fault on Feeder 1: (a) faulted feeder and (b) healthy feeder

C. HIL Test Results

In this section, a sub-set of test cases from the resonant-grounded scenario is selected to be discussed in more details. This sub-set of results has been selected in a manner that important observations and findings are highlighted. Table II provides selected test results for the full-compensation scenario (resonant grounding); similar tests were also carried out for under- and over-compensation scenarios, but dues the limited space, the results are not presented in this paper. However, an overview of all findings is presented in Section V.

Neutral voltage is not usually zero in a typical distribution substation due to normal system imbalance. The TGFD function starts when the neutral voltage rises above a threshold. Neutral voltage in normal operating condition should be considered when setting the neutral voltage trigger of the TGFD. The threshold should be higher than the normal neutral voltage of the system and lower than the voltage expected in case of high-impedance fault.

1) Solid Fault on Feeder 1 - R_f=0.01Ω (Case ID 1001)

In this case, a solid single-phase-to-ground (AG) fault is simulated on Feeder 1 (POW is set at 0 to represent the result of a worst-case scenario). Upon the occurrence of the fault, the system neutral voltage increases significantly which works as the trigger for the TGFD function.

Figure 8(a) shows the transient real and reactive power measured by the relay on Feeder 1 (faulted feeder). This figure

Table III- A summary of minimum fault current (maximum fault impedance) detected by TGFD

Affected Phase	Resonant-Grounded		92% Compensated		120% Compensated		Worst Cases	
	Z_f (kΩ)	I_f (A_{RMS})	Z_f (kΩ)	I_f (A_{RMS})	Z_f (kΩ)	I_f (A_{RMS})	Z_f (kΩ)	I_f (A_{RMS})
A	10	0.485	7.5	0.78	7.0	0.85	7.0	0.85
B	8	0.61	7.5	0.82	7.0	0.77	7.0	0.77
C	7	0.73	7.5	0.83	7.0	0.79	7.0	0.79

also indicates different pickup and operation signals of the relay including TGFD trigger ('TGFD_1_START'), TGFD forward operation ('TGFD_1_FORWARD'), and TGFD reverse operation ('TGFD_1_REVERSE'). As can be observed in this figure, subsequent to the fault, the TGFD function is triggered; further, since the fault is solid (Rf =0.01Ω), a negative reactive power is measured by the relay which causes the relay to detect a forward fault [4] correctly (in about 11ms). It is noted that, in this case, the TGFD function makes decision based on transient reactive power (transient Q) and does not switch to transient active power (transient P) mode; this is because transient Q is large enough (in magnitude) to exceed its negative threshold.
Figure 8(b) shows the transient P and Q measured by the relay of the healthy feeder (Feeder 2). The transient P and Q measured by this relay are positive and above their respective thresholds, indicating a healthy feeder. The decision in this test case is made base on the transient Q since its value is large and assertive.

2) High-Impedance Fault on Feeder 1- Rf=10kΩ (Case ID 1006)

Let us consider an AG High-Impedance Fault (HIF) on Feeder 1. Figure 9(a) shows the transient P and Q measured by Feeder 1 relay (faulted feeder). As can be observed in this figure, the TGFD function have operated based on transient P since the amount of transient Q is insignificant. In case of a HIF, the transient reactive power measured at 264Hz is normally small and does not reach its threshold to determine the fault direction. Therefore, the TGFD function switches to transient P and operates based on this quantity.
Figure 9(b) shows the transient P and Q recorded by the relay on Feeder 2 (Healthy feeder) while a HIF happens at the Feeder 1. As shown in the figure, both the transient active and reactive power are too small to define the fault direction. For such cases, the healthy feeder's relay uses "SmallPQ" function and announces a reverse fault after 500ms. "SmallPQ" function is incorporated in the TGFD algorithm to make a reverse direction decision when both transient P and Q are too small and do not reach their respective thresholds.
As stated before, more than 140 cases were tested in this study. A summary of results/finding is provided in Table III. As shown in this table, the TGFD function is capable of detecting fault currents as low as $0.85A_{RMS}$ in a typical utility distribution substation. The minimum fault current detected by the TGFD function was as low as $0.485A_{RMS}$ in some test cases, depending on the compensation level, system imbalance, and point on wave.

V. CONCLUSIONS AND RECOMMENDATIONS

This paper presented the operating principles of the Transient Ground Fault Detection (TGFD) function in compensated-grounded systems. The effectiveness of this function was verified using HIL testing on a pilot utility project. The results demonstrated satisfactory performance of the TGFD function for very low fault currents in a resonant-grounded system. The following is a list of conclusions and recommendations based on the results of this study:

- To detect low fault currents, it is important to intelligently select the CT ratio, type, and accuracy. For fire mitigation applications, lower CT ratios with the accuracy of 0.3% or better is recommended.
- The minimum fault current that the relay can detect is a function of the system characteristics (i.e., line charging current and its resistive component).
- As the compensation level drifts from the full-resonance level, the neutral voltage rise will be affected. It is important to ensure the system works close to the full compensation level.
- The minimum fault current detected by the relay (maximum fault resistance) depends on the compensation level. To reach lower fault current detection, the system should be as close as possible to full-resonance compensation.
- Depending on the affected phase (A, B, or C), the TGFD may detect lower fault current. This is due to the system voltage imbalance under normal condition.
- The guaranteed minimum fault current that could be detected by the TGFD in this study system (worst-case scenario including incomplete compensation and system imbalance) is about 0.85A.

ACKNOWLEDGEMENT

This project was funded by Southern California Edison (SCE) through Electric Program Investment Charge (EPIC) program of the California Public Utilities Commission (CPUC).

REFERENCES

[1] T. Marxsen, "Analysis of resonant earthed networks," Marxsen Consulting Pty Ltd, 2015.

[2] H. Hengxu and C. Liu, "Ground fault direction determination for medium or high voltage distribution networks". Patent EP 2 741 389 B1, 12 10 2012.

[3] K. Venkataraman, B. Kirby, H. Ha and P. Newman, "Transient Earth Fault Detection on Compensated Earthed System," 2013.

[4] "F60 Feeder Protection Sysstem Instuction Manual, Product version: 8.0x, GE publication code: 1601-0093-AJ2 (GEK-134143A)," GE Grid Solutions.

[5] T. Marxsen, "Powerline Bushfire Safety Program, REFCL Technologies Test Program – Final Report," Victoria State Governmentpp, Victoria, Australia, 2015.

Hasan Bayat received his Ph.D in Electrical Engineering from the University of Western Ontario, Canada, in 2018. He has more than seven years of academic and industrial work experience in power system studies, and specializes in grid integration of distributed energy resources including modelling, control, and analysis of power conversion systems; power system protection and control (P&C); power system transient and dynamic studies; and microgrid control, automation, and protection. He is a reviewer for IEEE Transactions on Energy Conversion and Power Delivery.

Tirath Bains completed his M.Sc. (Power Systems) in 2014, and Ph.D (Power Systems) in 2018 both at the University of Western Ontario, Canada. He worked at the Alstom India limited from 2008 to 2009. Currently, he is with GE Grid Solutions, Canada, as a Customer Application Engineer. His research interest includes fault location in transmission lines (impedance based and traveling-wave based), detection of high impedance faults, and distance protection.

Amin Zamani is the Director of the Global Grid Modernization Center of Excellence at GE Grid Solutions. He has more than 10 years of professional experience and specializes in the power system protection and control; modelling and analysis of power systems; distributed generation integration; and microgrids. He has worked on several utility and industrial projects focusing on microgrid development, DER integration, distribution automation, and advanced protection schemes. Amin is a Senior Member of IEEE and serves as the vice chair of C25 working group; he is a Professional Engineer in the province of Ontario.

Matthew Webster is working as a Senior Engineer at Southern California Edison Company (SCE). He has worked at SCE for ten years in the Protection Engineering Department. He received his Bachelor's degree at California State Polytechnic University, Pomona. He received his Master's degree in Power and System's Engineering at California State University, Los Angeles.

Jesse Rorabaugh is working as a Senior Engineer at Southern California Edison Company (SCE). He received his Bachelor's degree at Fresno State with a triple major in Physics, Chemistry, and Biology then a Master's degree at Cornell in Biomedical Engineering and a Professional Engineer license as an Electrical Engineer in the State of California. He is an active IEEE member and serves as chair for the G4 working group responsible for IEEE Std. 1246 and 1268 and vice chair for the G9 working group responsible for IEEE Std. 837.

Arturo Torres received his Bachelor's degree in Electrical Engineering (Power System) from California State University, Los Angeles. He is currently employed with Southern California Edison Company (SCE) as a Senior Protection Engineer with in Protection Asset Engineering group. Arturo has more than 20 years of experience in the power system protection engineering.